Proceedings of the
44th IEEE Conference on Decision and Control, and
the European Control Conference 2005
Seville, Spain, December 12-15, 2005

Maximum A Posteriori Estimation of Energetics in Silicon Self-diffusion

Charlotte T. Kwok, Kapil Dev, Edmund G. Seebauer, and Richard D. Braatz, *Senior Member*, *IEEE*

Abstract—**Maximum A Posteriori (MAP) estimation was employed to refine estimates of various energetics in silicon self-diffusion. Self-diffusion profiles were augmented with prior parameter estimates determined from previous experimental systems to obtain improved values. Parameter sensitivity analysis was utilized before MAP estimation to determine the relative importance of model parameters. The sensitivities were a strong function of the surface boundary condition. For conditions with high surface loss flux, the energy for exchange between an interstitial and the lattice is the most critical. For conditions with a low surface loss flux, the dissociation energy of large-atom clusters plays a more important role. The incorporation of information from the new experimental system substantially improved the estimates of parameters that could not be identified accurately in previously studied systems.**

I. Introduction

THE mechanism of diffusion in silicon has been extensively investigated in the past few decades [1]. One of the major driving forces comes from the technological need to understand and control the transient enhanced diffusion (TED) [2]-[3] of implanted atoms during annealing, which is a major roadblock to the continuous miniaturization of semiconductor devices. Although it is generally accepted that point defects such as interstitials and vacancies serve as primary mediators in silicon diffusion [4], these defects are difficult to monitor directly owing to their low concentrations, making the study of the diffusion mechanism very challenging.

To elucidate this problem, models have been employed with experimental data to estimate the various energetics of diffusion and reaction of species in silicon [5]-[8]. In the most data-efficient implementations, model identification is an iterative process involving optimal experimental design, experimental data collection, parameter estimation, and hypothesis mechanism selection, which are repeated until accurate parameter estimates are obtained [9]-[11]. However, even with the application of optimal experimental design, the accuracy of the parameter estimates may still be limited by the physicochemical behavior of the process and various practical constraints in experimentation. In this case, obtaining accurate estimates of the model parameters may require studying additional experimental systems. In other words, a model with high predictability may be achievable by combining the information from multiple experimental systems.

In previous work on solid state diffusion, we developed a model to describe the transient enhanced diffusion (TED) of boron in silicon [12]-[14]. Values of the model parameters were determined by parametric sensitivity analysis, maximum likelihood (ML) estimation, and maximum a posteriori (MAP) estimation. In addition to a good agreement between experimental and simulated boron concentration profiles, our model provided the first published agreement between model simulations and the "Sematech curve" [15], which generalizes experimental sheet resistance–junction depth pairs employing various experimental conditions.

In other recent work, we studied the photo-stimulated effect in silicon self-diffusion [16]. By utilizing a silicon isotope heterostructure, the activation energy for interstitial formation and diffusion with and without surface illumination and the energy barrier for the exchange reaction between interstitial and the lattice were determined.

In other prior work [17], we studied the effect of surface bond structure on the annihilation rate of self-interstitials. Isotopically-labeled ^{30}Si was implanted into a silicon matrix depleted in the isotope. The surface was saturated with nitrogen to various degrees before annealing. The effect of nitride coverage was quantified by the surface annihilation probability of silicon interstitials, which was determined by maximum likelihood (ML) estimation.

Although the aforementioned three systems possess different objectives, their models share similar elementary reactions, such as interstitial diffusion and clustering. This paper refines the common parameters among the models by augmenting data collected from the new experimental system to the prior information obtained from previously studied systems. This was accomplished using parameter sensitivity analysis and maximum a posteriori (MAP) estimation.

Parameter sensitivities quantify the variations in the model output in response to perturbations in its parameters. The relative importance of various parameters in the model indicates which parameters can be estimated most accurately and should be included in the parameter estimation algorithm. Maximum a posteriori (MAP) estimation determines the most likely values of model parameters when prior information is available. It utilizes Bayes theorem to determine the refined probability density function of the param-

Manuscript received February 22, 2005. This work was partially supported by NSF (CTS 02-03237). SIMS was performed at the Center for Microanalysis of Materials, University of Illinois, which is partially supported by the U.S. Department of Energy under grant DEFG02-96-ER45439.

R. D. Braatz is with the University of Illinois at Urbana-Champaign, Urbana, IL 61801 USA (phone: 217-333-5073; fax: 217-333-5052; e-mail: braatz@uiuc.edu).

C. T. Kwok, K. Dev, and E. G. Seebauer are with the Department of Chemical and Biomolecular Engineering, University of Illinois at Urbana-Champaign, Urbana, IL 61801 USA.

0-7803-9568-9/05/$20.00 ©2005 IEEE

eters by combining prior statistical information and additional experimental data. By utilizing MAP estimation, the prior information from previously studied systems were augmented with new experimental data to obtain refined estimates of various parameters.

II. Experimental Methods

The experimental system consists of isotopically-labeled ^{30}Si tracer implanted into an epitaxial matrix depleted in the ^{30}Si isotope. Experiments were performed in a turbomolecularly pumped ultrahigh vacuum chamber with a base pressure in the low 10^{-9} torr range. The Si-isotope heterostructure consists of a 4 μm thick slightly p-type ([B] = 10^{15} cm^{-3}) epitaxial Si depleted in ^{30}Si to 0.002% (compared to the natural abundance of 3.10%) grown on natural silicon, which was also doped with boron, but to a level of 10^{19} cm^{-3}. SiH_4 enriched in the ^{30}Si isotope to 90% was implanted into the Si matrix. Nitride coverage was accomplished by exposure to ammonia (99.99%) at 800°C. The degree of nitride coverage was measured by Auger Electron Spectroscopy (AES) and was controlled by exposure time.

Three samples were prepared. In sample 1 there was no ammonia exposure. In sample 2, the specimen was exposed to ammonia *before* ion implantation to give nitride coverage of about 1 monolayer. In sample 3, after nitride growth and ion implantation identical to that of sample 2, there was a further nitride growth of about 1 monolayer *after* ion implantation. The samples were soak-annealed by resistive heating at 1000°C for 120 min for sample 1 and at 980°C for 90 min for samples 2 and 3.

The as-implanted and annealed profiles were measured *ex situ* by a dual beam Tof-SIMS instrument. Sputtering was accomplished by a Cs^+ ion beam at 2 keV and 60 nA, and the analysis was made by using a Au^+ ion beam at 22 keV and 600 pA. The ion count of ^{30}Si was converted to concentration by calibrating to the signal of ^{28}Si, whose concentration is known.

III. Silicon Self-diffusion Model

The model depicts the diffusion of implanted ^{30}Si tracer in the expitaxial Si matrix depleted in the ^{30}Si isotope, as described elsewhere [17]. It utilizes continuum equations to describe the reaction and diffusion of interstitial atoms and related defects in silicon. These equations have the general form for species i:

$$\partial C_i / \partial t = -\partial J_i / \partial x + G_i \tag{1}$$

where C_i, J_i, and G_i denote the concentration, flux, and net generation rate of species i, respectively. The effect of the electric field on the flux J_i is negligible considering that the sample is weakly and uniformly doped. The net generation term G_i incorporates terms associated with cluster formation and exchange between interstitials and the lattice. The reactions for the clustering of interstitials in the model are

$$I_{m-1} + I \leftrightarrow I_m, \quad 2 \le m \le 5 \tag{2}$$

where the index m denotes the size of (that is, the number of atoms in) the cluster. The maximum cluster size is restricted to five owing to the number of equations that can be solved by the simulator. The exchange between interstitial silicon and the lattice is the reaction

$$^{30}Si_i + {}^{28}Si_l \leftrightarrow {}^{30}Si_l + {}^{28}Si_i \tag{3}$$

The effect of adsorbate coverage on the surface annihilation rate of interstitials is quantified by the surface loss probability S, which is incorporated in the boundary condition as

$$-D\,\partial C/\partial x\big|_{x=0} = J_{total}\,S \tag{4}$$

where J_{total} denotes the total impinging flux of interstitials. The actual flux at the surface is the product of the total impinging flux and the surface loss probability.

The model was implemented using the process simulator FLOOPS [18]. The initial condition for each simulation run was an experimental as-implanted profile, with the assumption that 20% of the implanted ^{30}Si enters as substitutional sites. The initial condition for the interstitial ^{28}Si was set based on the "+1 model" [19]. Values of surface loss probability S at different degrees of nitrogen coverage were determined by maximum likelihood (ML) estimation with S as the only adjustable parameter. Fig. 1 shows the experimental as-implanted and annealed profiles as well as the simulation fit for three sets of conditions. The sample with highest nitrogen coverage (sample 3) shows the most profile spreading, while the clean surface sample (sample 1) shows the least. The ML estimates of the surface loss probability S and the values of key activation energies are summarized in Table I. The more diffused profile corresponds to a smaller surface loss probability S.

The values of key activation energies employed in the

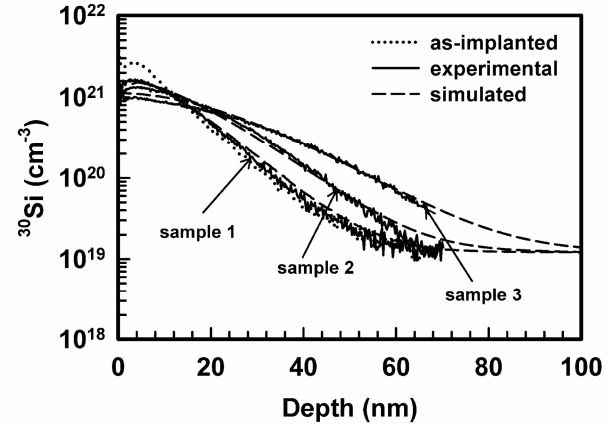

Fig. 1. Experimental and simulated ^{30}Si profiles using the surface loss probability S as the only adjustable parameter determined by maximum likelihood (ML) estimation.

model were determined by maximum likelihood (ML) estimation and maximum a posteriori (MAP) estimation from other experimental systems [12]-[14], [16]. Accuracy of the estimates was limited by the sensitivity of the measured simulation profile to these parameters. Here parameter sensitivity analysis and MAP estimation are used to obtain

refined estimates by augmenting the prior information with new experimental data.

IV. System Tools

A. Parameter Sensitivity Analysis

Parameter sensitivity analysis quantifies the influence of perturbations in model parameters on the process outputs. This technique has been widely applied in analysis and design of chemical systems [20]-[21]. The analysis determines which model parameters need to be estimated or calculated most accurately in order to give high predictability, and which can be largely ignored. The parameters with high sensitivities to measurements can be determined most accurately by parameter estimation. The matrix F of sensitivities includes the partial derivatives of the variables β_j with respect to the dependent variables P_i [22],

$$F_{i,j} = F(P_i;\beta_j) = \partial P_i(\beta_j)/\partial\beta_j\,, \tag{5}$$

where $F(P_i, \beta_j)$ denotes the sensitivity of the i^{th} measurement to the j^{th} parameter.

This laboratory has applied sensitivity analysis to study the relative contribution of various activation energies in the transient enhanced diffusion (TED) of boron in silicon [12]. The results suggested that the activation energies most important in the boron model are those for interstitial boron diffusion, kick-in, and the dissociation of the $(B_s\text{-}Si_i)^+$ intermediate to liberate either interstitial B (kick-out) or Si. As the silicon self-diffusion system shares similar elementary reactions with the boron model (e.g., interstitial diffusion and cluster dynamics), some of the activation energies in the silicon self-diffusion model are the same as for the boron system (see Table I). However, as the parameter sensitivities are a function of the process and the corresponding experimental conditions, parameters that are relatively insensitive in one system may be important in another. In this case, the accuracy of some of the parameter estimates can be improved by combining the information from multiple experimental systems.

Both the boron TED system and the silicon self-diffusion system entail the diffusion of species under supersaturation of defects. However, the two systems are different in several ways. One major difference lies on the boundary condition. In the boron system, the silicon surface was covered with screen oxide during experiment, giving a boundary condition reasonably close to a perfect reflector (i.e., $S = 0$). For the self-diffusion model, the surface dangling bonds were saturated with adsorbate to give a boundary condition lying between the two extremes of perfect sink and perfect reflector.

The annealing program employed was different, too. The boron experiment utilized a spike anneal program. The sample was heated up and cooled down rapidly such that it was kept at high temperature (>600°C) for short time (~20 s). Soak anneal was used in the self-diffusion experiment, which kept the sample at high temperature for much longer time (~90 min).

The differences between the two systems may result in large differences in the sensitivities of the model outputs to the same model parameter. For example, the soak anneal program employed in the self-diffusion model would be expected to improve the sensitivities of model outputs to parameters involved in the reaction and diffusion that have larger time constants, while the difference in the boundary condition may result in a change of the dominating reaction/diffusion mechanism in the system.

TABLE I
Maximum likelihood (ML) estimates of the surface loss probability S and values of key activation energies

Parameter	Value	Standard deviation	Method	Ref
E_2 (cluster dissociation – size 2)	1.4 eV	0.03	ML	14
E_3 (cluster dissociation – size 3)	2.192 eV	0.012	MAP	14
E_4 (cluster dissociation – size 4)	3.055 eV	0.002	MAP	14
E_5 (cluster dissociation – size 5)	3.7 eV	0.1	ML	14
E_{diff} (Si interstitial diffusivity)	0.72 eV	0.03	ML	14
E_{ex} (exchange between interstitial and substitutional Si)	1.02 eV	0.3	ML	16
S_1 (surface loss probability, sample 1)	4.15×10^{-2}	3.44×10^{-3}	ML	17
S_2 (surface loss probability, sample 2)	7.11×10^{-4}	5.36×10^{-6}	ML	17
S_3 (surface loss probability, sample 3)	2.36×10^{-4}	1.18×10^{-6}	ML	17

In this work, the sensitivities were estimated by the finite difference method:

$$F(P_i;\beta_j) \approx \frac{\Delta P_i}{\Delta\beta_j} = \frac{P_i(\beta_j+\Delta\beta_j) - P_i(\beta_j-\Delta\beta_j)}{2\Delta\beta_j}. \tag{6}$$

The total sensitivity for the j^{th} parameter, Φ_j, is given by the sum of squares of this approximated partial derivative over the entire depth of the ^{30}Si profile weighed by the corresponding measurement covariance at the i^{th} depth, σ_i^2,

$$\Phi_j = \sum_{i=1}^{N_d} \frac{1}{\sigma_i^2}\left(\frac{C^{\,^{30}Si}_{i,\beta_j+\Delta\beta_j} - C^{\,^{30}Si}_{i,\beta_j-\Delta\beta_j}}{2\Delta\beta_j}\right)^2, \tag{7}$$

where N_d denotes the total number of data points in the ^{30}Si profile, and $\Delta\beta_j/\beta_j = 0.1$. A higher value of the total sensitivity Φ_j implies a stronger influence of the corresponding model parameter β_j on the final ^{30}Si profile. The data points with smaller measurement covariance are weighed stronger in determining the total sensitivity. The standard deviation at each depth σ_i was estimated by the measurement of n different SIMS profiles on the same specimen, yielding

$$\sigma_i = \frac{1}{n-1}\sqrt{\sum_{m=1}^{n}(C_{i,m} - \hat{C}_i)^2} \tag{8}$$

where $\hat{C}_i$ is the average concentration over the n measurements for the i^{th} depth. The standard deviation on a relative basis (*i.e.*, normalized by concentration) obeyed the following square-root relation:

$$\sigma_i / \hat{C}_i = k_2 + k_1 / \sqrt{\hat{C}_i} \ . \tag{9}$$

where k_1 and k_2 denote constants equal to 4.4×10^{8} and 2.7×10^{-2}, respectively. Equation (9) indicates that the relative measurement error decreased with the square root of the signal strength.

As experiments were performed under various degrees of adsorbate coverage, the sensitivity analysis was repeated for various values of the surface loss probability *S*. This helped elucidate the effect of surface boundary condition on the governing diffusion/reaction mechanism in the system. The results also can be used to guide experimental design if particular parameters need to be refined in future studies.

B. Maximum a posteriori (MAP) Estimation

Maximum a posteriori (MAP) estimation determines the most likely values of parameters when prior information is available [23]-[24]. MAP estimation optimally combines prior statistical information of the parameter estimates with additional experimental data to obtain improved *a posteriori* estimates. For this application MAP estimation can be equivalently posed as a minimization problem,

$$\min_{\substack{\bar{\beta},S_k \\ k=1,\cdots,d}} \left\{ \begin{array}{l} \left(\bar{\beta}-\mu\right)^{\mathrm{T}} V_{\mu}^{-1}\left(\bar{\beta}-\mu\right)+ \\ \qquad \sum_{k=1}^{d}\left(Y_k-P_k(\bar{\beta},S_k)\right)^{\mathrm{T}} V_{\varepsilon,k}^{-1}\left(Y_k-P_k(\bar{\beta},S_k)\right) \end{array} \right\} \tag{10}$$

where $\bar{\beta}$ denotes the vector of estimated parameters that are the same for all profiles, μ is the vector of corresponding *a priori* parameter estimates, V_μ is the prior parameter covariance matrix, *d* is the total number of SIMS profiles, and S_k is the surface loss probability, Y_k is the vector of experimental observations, P_k is the vector of model predictions, and $V_{\varepsilon,k}$ is the measurement covariance matrix for the k^{th} profile. Assuming the measurement errors at different depths are uncorrelated, the measurement covariance matrix is diagonal with nonzero elements given by

$$\left[V_{\varepsilon,k}\right]_{ii} = \sigma_{i,k}^2 \tag{11}$$

where σ_i is determined by

$$\sigma_{i,k} / C_{i,k} = k_2 + k_1 / \sqrt{C_{i,k}} \ . \tag{12}$$

Assuming the accuracies of the individual prior parameter estimates are independent of each another, the prior parameter covariance matrix can be expressed as a diagonal matrix with nonzero entries given by

$$V_{\mu,jj} = \sigma_{\bar{\beta}_j}^2 \tag{13}$$

where $\sigma_{\bar{\beta}_j}$ is the standard deviation in the prior estimate of the j^{th} parameter. No prior information was assumed for the surface loss probability S_k, which varies with the adsorbate coverage that is different for each profile. In the case where only the surface loss probabilities are estimated, (10) gives maximum likelihood estimates.

The parameters to estimate in $\bar{\beta}$ is chosen based on the results of sensitivity analysis such that parameters with low sensitivities are not included. The objective function in (10) is formulated as the sum of weighed squared differences between the experimental profile concentrations and the model predictions for *all* available profiles. The values of various activation energies in $\bar{\beta}$ are independent of the experimental conditions, while the values of S_k are a function of nitride coverage.

All of the estimated parameters can be stacked into a single vector,

$$\beta = [\bar{\beta}\ S_1 \cdots S_d]^{\mathrm{T}}, \tag{14}$$

with an estimate of the covariance of $(\beta^* - \beta_{true})$ given by

$$\operatorname{cov}(\beta^*-\beta_{true}) = V_{\beta^*} \approx \left(F^{\mathrm{T}} \begin{pmatrix} V_{\varepsilon,1} & 0 & 0 \\ 0 & \ddots & 0 \\ 0 & 0 & V_{\varepsilon,d} \end{pmatrix}^{-1} F + \begin{pmatrix} V_{\mu}^{-1} & 0 \\ 0 & 0 \end{pmatrix} \right)^{-1} \tag{15}$$

where β^* and β_{true} denote the best estimate and the true value of the vector of parameters, respectively, and each 0 is a matrix of zeros of compatible dimensions. The matrix *F* is the sensitivity matrix of

$$P = [P_1 \cdots P_d]^{\mathrm{T}} \tag{16}$$

with respect to the vector of parameters β, computed from (6).

The accuracy of the parameter estimates are quantified by a hyperellipsoidal confidence region given by

$$E_\beta = \left\{ \beta : (\beta-\beta_{true}) V_{\beta^*}^{-1} (\beta-\beta_{true}) \le \chi_\alpha^2(p) \right\} \tag{17}$$

where α denotes the confidence level and χ denotes the chi-squared distribution with *p* degrees of freedom. The confidence region can be visualized by confidence intervals:

$$\beta_j^* - \sqrt{\chi_\alpha^2(p) V_{\beta^*,jj}} \le \beta_{true,j} \le \beta_j^* + \sqrt{\chi_\alpha^2(p) V_{\beta^*,jj}} \tag{18}$$

The confidence intervals are a poorer representation of the hyperellipsoidal confidence region when the off-diagonal elements in V_{β^*} are large relative to its diagonal elements, in which case the correlation between the parameters is significant.

V. Results and Discussion

A. Sensitivity Analysis

Values of the total sensitivities for different surface loss probabilities are shown in Table II. Results can be summarized as follows:

1) The energetics of exchange between interstitial and substitutional silicon, E_{ex}, have a large influence on the final concentration profile for high values of the surface loss probability *S* (10^{-2} and 10^{-4}). The total sensitivity decreases as *S* decreases.
2) The total sensitivities of cluster energetics mostly increase as *S* decreases. For small *S* (10^{-6} and 10^{-8}), the profile is most sensitive to the cluster energetics for

large clusters (E_4 and E_5).

3) The profile is sensitive to E_{diff} over the entire range of the surface loss probability S.

An explanation of the above results requires a deep understanding of the self-diffusion mechanism. In Si implanted to significant levels of interstitial supersaturation as described above, the self-diffusion behavior is determined primarily by the interplay between the interstitials, the surface, and the reservoirs that render interstitials immobile, *i.e.*, lattice sites and interstitial clusters. A high value of the surface loss probability S implies a high flux at the surface. As interstitials of both ^{28}Si and ^{30}Si move towards the surface, interstitial ^{30}Si will be selectively immobilized by the exchange reaction with lattice sites described in (3), owing to a higher concentration of substitutional ^{28}Si than ^{30}Si. Continuous removal of the interstitial ^{28}Si at the surface drives the exchange reaction to the right hand side, resulting in more ^{30}Si kicked into lattice sites. Owing to this selective removal of interstitial ^{28}Si over ^{30}Si, a high value of the surface loss probability S results in a less diffused final ^{30}Si profile (see Fig. 1). This also explains why the profile is very sensitive to the activation energy for the kick-in reaction (E_{ex}) for high values of the surface loss probability S.

As the value of the surface loss probability S decreases, the effect of surface removal decreases, and the interstitials tend to diffuse to the bulk rather than the surface. The exchange reaction becomes less important in freezing the ^{30}Si profile, because of the relatively high concentration of interstitial ^{28}Si present in the bulk. Clusters then become a more effective reservoir for interstitials.

The magnitude of the total sensitivity for E_{diff} agrees with physical intuition. It is reasonable to expect that the diffusivity of the silicon interstitial would play an important role on the final annealed profile regardless of the mechanism that render interstitials immobile. Hence the total sensitivity of E_{diff} is high for all values of the surface loss probability S.

Based on the results of ML estimation with the surface loss probability S as the only adjustable parameter (see Table I), the available experimental data gave values of the surface loss probability S between 10^{-4} and 10^{-1}. In this regime, the concentration profiles are relatively insensitive to the dissociation energy of small clusters (see Table II). As a result, E_2 and E_3 were not included in the parameter set for maximum a posteriori estimation, resulting in the vector of parameter estimates defined by

$$\beta^{\mathrm{T}} = \left[E_4, E_5, E_{ex}, E_{diff}, S_1, S_2, S_3 \right]^{\mathrm{T}}. \tag{19}$$

According to the results of the sensitivity analysis (see Table II), if the values of E_2 and E_3 need to be determined more accurately in the future, then the experiments should be performed under conditions in which the surface boundary condition is close to that of a perfect reflector, that is, experimental conditions in which the surface loss probability S is small.

Note that the concentration profile was not very sensitive to E_5 and E_{diff} in previous experimental systems (which is why the standard deviations from past parameter estimation studies are relatively large in Table I), but the concentration profiles are very sensitive to these parameters in the present system (see Table II). This indicates that incorporating the experimental results from the present system with prior information should result in more accurate estimates of these parameters.

The dissociation energy of the second largest cluster, E_4, shows moderate sensitivity for $S \approx 10^{-4}$ (see Table II). Although a prior parameter estimation study for boron diffusion experiments estimated a standard deviation of 0.002 for the estimate of this parameter, this value is too small for use in the MAP estimation for this silicon self-diffusion study. In the boron system, there are three kinds of clusters, namely pure B clusters, pure Si clusters, and mixed B-Si clusters. The dissociation energy for clusters of size bigger than 2 was assumed to be solely size-dependent. This assumption is probably only an approximation. Results from first-principles calculations [25] and the tight-binding method [26] indicate that the identity of atoms in a cluster affects the value of the formation energy. In addition, it is unlikely that the dissociation of these three groups of clusters is of same importance in affecting the final boron profile. The estimated high accuracy of the estimate of E_4 may be due to a high sensitivity of the concentration profiles to the dissociation of a *certain* group of clusters. These issues suggest that the prior standard deviation for E_4 used in the current MAP estimation should be increased; we used 0.1 eV, which is the same as that of E_5. This makes the refined *a posteriori* estimate of E_4 a more defensible value for pure Si clusters. In the next section the refined value is compared to the prior estimate to quantify the validity of the "size-dependent-only" assumption.

B. Maximum a posteriori (MAP) Estimation

MAP estimates of the model parameters and the associated 95% confidence intervals are shown in Table III. Fig. 2 shows the simulated profiles using the refined parameters. The simulated profiles with MAP estimates are closer to the experimental profiles than when *a priori* estimates are used (see Fig. 1), especially for the clean surface sample (sample 1). Values of the MAP estimates are reasonably close to the prior estimates, but with confidence intervals significantly tightened. With the exception of E_4, each estimate lies within the 95% confidence region of the prior estimate, suggesting that the values of the model

TABLE II
VALUES OF THE TOTAL SENSITIVITIES OF MODEL PARAMETERS AT VARIOUS VALUES OF THE SURFACE LOSS PROBABILITY S

Parameter	Total Sensitivity for the j^{th} parameter, Φ_j			
	$S = 10^{-2}$	$S = 10^{-4}$	$S = 10^{-6}$	$S = 10^{-8}$
E_2	3.87×10	1.20×10	2.87×10^{4}	4.27×10^{5}
E_3	1.91×10	6.15×10	5.60×10^{4}	4.41×10^{5}
E_4	2.74×10	5.24×10^{4}	1.54×10^{6}	5.74×10^{5}
E_5	1.41×10^{3}	4.27×10^{5}	4.97×10^{6}	6.62×10^{6}
E_{diff}	1.69×10^{6}	2.41×10^{5}	2.75×10^{4}	4.36×10^{5}
E_{ex}	1.91×10^{6}	2.65×10^{5}	2.64×10^{2}	1.96×10^{2}

parameters are consistent in the various experimental systems studied.

As discussed above, the error bound in the prior estimate of E_4, the dissociation energy of the second largest clusters, was loosened in present study. The refined MAP estimate is larger than the prior estimate and is outside the original confidence interval. This discrepancy suggests that dissociation of clusters may not be solely dependent on the number of atoms in the cluster. In order to obtain a more defensible value for cluster energetics, refinement in the boron model and additional experiments may be necessary.

TABLE III
MAXIMUM A POSTERIORI (MAP) ESTIMATES OF THE SURFACE LOSS PROBABILITY S AND VARIOUS ACTIVATION ENERGIES

Parameter	MAP Estimate	95% Confidence Interval Half-width
E_4	3.1087 eV	0.0183
E_5	3.7749 eV	0.0059
E_{diff}	0.7642 eV	0.0053
E_{ex}	0.9636 eV	0.0051
S_1	6.72×10^{-2}	5.71×10^{-4}
S_2	5.77×10^{-4}	6.64×10^{-6}
S_3	2.19×10^{-4}	1.87×10^{-6}

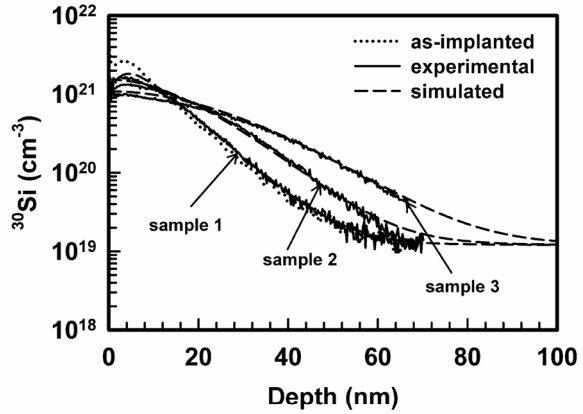

Fig. 2. Experimental and simulated ^{30}Si profiles using refined estimates of the surface loss probability S and various energetics determined by maximum a posteriori (MAP) estimation.

VI. CONCLUSIONS

The energetics in silicon self-diffusion were identified using a combination of parametric sensitivity analysis and maximum a posteriori (MAP) estimation. Refined parameter estimates with tighter confidence intervals were obtained by combining information from multiple experimental systems. The much higher sensitivity of the concentration profiles in the new experimental system to the dissociation energy of the largest clusters E_5 and the energetics of Si interstitial diffusion E_{diff} enabled an order-of-magnitude improvement in the accuracy of the estimates of these parameters, upon application of MAP estimation. The greatest improvement in accuracy was for the activation energy for the exchange between interstitial and substitutional silicon, E_{ex}, which had a very strong effect on the concentration profiles for high values of the surface loss probability S. The results suggest that the dissociation energy of the second largest clusters may be dependent on composition as well as the number of atoms in the clusters.

ACKNOWLEDGMENT

We thank Steve Burdin at Isonics Corporation for overseeing the successful creation of isotopically-labeled specimens and Joel Ager at Lawrence Berkeley National Laboratories for arranging the supply of isotopically-labeled silane.

REFERENCES

[1] P. M. Fahey, P. B. Griffin, and J. D. Plummer, *Rev. Mod. Phys.*, vol. 61, pp. 289-384, Apr. 1989, and references therein.
[2] S. C. Jain, W. Schoenmaker, R. Lindsay, P. A. Stolk, S. Decoutere, M. Willander, and H. Maes, *J. Appl. Phys.*, vol. 91, pp. 8919, 2002.
[3] L. Shao, J. Liu, Q. Y. Chen, and W. Chu, *Materials Science and Engineering R*, vol. 42, pp. 65-114, Nov. 2003.
[4] H. Bracht, E. E. Haller, and R. Clark-Phelps, *Phys. Rev. Lett.*, vol. 81, pp. 393-396, Jul. 1998.
[5] P. A. Stolk, et al., *J. Appl. Phys.*, vol. 81, pp. 6031-6050, May 1997.
[6] H. Bracht, N. A. Stolwijk, and H. Mehrer, *Phys. Rev. B*, vol. 52, pp. 16542-16560, Dec. 1995.
[7] S. Chakravarthi and S. T. Dunham, *J. Appl. Phys.*, vol. 89, pp. 3650-3655, Apr. 2001.
[8] N. E. B. Cowern, K. T. F. Janssen, G. F. A. van de Walle, and D. J. Gravesteijn, *Phys. Rev. Lett.*, vol. 65, pp. 2434-2437, Nov. 1990.
[9] E. Walter and L. Pronzato, *Automatica*, vol. 26, pp. 195-213, 1990.
[10] A. F. Emery and A. V. Nenarokomov, *Meas. Sci. Technol.*, vol. 9, pp. 864-876, Jun. 1998.
[11] R. D. Braatz, R. C. Alkire, E. Seebauer, E. Rusli, R. Gunawan, T. O. Drews, X. Li, and Y. He, in *Int. Symp. on Dynamics and Control of Process Systems*, Cambridge, MA, Paper 96, Jul. 2004.
[12] R. Gunawan, M. Y. L. Jung, R. D. Braatz, and E. G. Seebauer, *J. Electrochem. Soc.*, vol. 150, pp. G758-G765, Dec. 2003.
[13] M. Y. L. Jung, R. Gunawan, R. D. Braatz, and E. G. Seebauer, *AIChE J.*, vol. 50, pp. 3248-3256, Dec. 2004.
[14] R. Gunawan, M. Y. L. Jung, E. G. Seebauer, and R. D. Braatz, *AIChE J.*, vol. 49, pp. 2114-2123, Aug. 2003.
[15] B. Murto, in *Proc. of the Third National Implant Users Meeting*, Austin, TX, Oct. 1999.
[16] R. Vaidyanathan, M. Y. L. Jung, R. D. Braatz, and E. G. Seebauer, U. of Illinois at Urbana-Champaign, IL 61801, USA, technical report.
[17] C. T. M. Kwok, K. Dev, R. D. Braatz, and E. G. Seebauer, U. of Illinois at Urbana-Champaign, IL 61801, USA, technical report.
[18] M. Law, U. of Florida at Gainesville, http://www.swamp.tec.ufl.edu/.
[19] M. D. Giles, *J. Electrochem. Soc.*, vol. 138, pp. 1160-1165, 1991.
[20] J. R. Leis, S. A. Gallagher, and M. A. Kramer, *Comp. Chem. Eng.*, vol. 11, pp. 409-421, 1987.
[21] F. D. Van Voorhees and A. Terry Bahill, in *Proc. of the IEEE Int. Conf. on Systems, Man and Cybernetics*, vol. 2, Vancouver, Canada, Oct. 1995, pp. 971-976.
[22] R. Tomović and M. Vukobratović, *General Sensitivity Theory*. New York: Elsevier, 1972, ch. 1.
[23] J. V. Beck and K. J. Arnold, *Parameter Estimation in Engineering and Science*. New York: Wiley, 1977, ch. 5-7.
[24] G. Sparacino, C. Tombolato, and C. Cobelli, *IEEE Trans. on Biomedical Engineering*, vol. 47, pp. 801-811, Jun. 2000.
[25] T. J. Lenosky, B. Sadigh, S. K. Theiss, M. Caturla, and T. D. Rubia, *Appl. Phys. Lett.*, vol. 77, pp. 1834-1836, Sept. 2000.
[26] W. Luo and P. Clancy, *J. Appl. Phys.*, vol. 89, pp. 1596, Feb. 2001.